Pergamon

Journal of the Mechanics and Physics of Solids
49 (2001) 149–171

JOURNAL OF THE MECHANICS AND PHYSICS OF SOLIDS

www.elsevier.com/locate/jmps

Dynamics of chains with non-monotone stress–strain relations. II. Nonlinear waves and waves of phase transition

Alexander M. Balk [a], Andrej V. Cherkaev [a,*], Leonid I. Slepyan [b]

[a] *Department of Mathematics, University of Utah, Salt Lake City, UT 84112, USA*
[b] *Department of Solid Mechanics, Materials and Structures, Tel Aviv University, Tel Aviv, Israel*

Received 10 May 1999; received in revised form 28 February 2000

Abstract

We investigate the dynamics of a one dimensional mass-spring chain with non-monotone dependence of the spring force vs. spring elongation. For this strongly nonlinear system we find a family of exact solutions that represent nonlinear waves. We have found numerically that this system displays a dynamical phase transition from the stationary phase (when all masses are at rest) to the *twinkling* phase (when the masses oscillate in a wave motion). This *transition* has two fronts which propagate with different speeds. We study this phase transition analytically and derive relations between its quantitative characteristics. © 2000 Elsevier Science Ltd. All rights reserved.

Keywords: A. Phase transformations; A. Dynamics; Variational principles; B. Constitutive behaviour

1. Introduction

1.1. The system

We consider the dynamics of a one-dimensional chain of masses m connected by identical springs (see Fig. 1). This system is described by the following equations

$$\rho\ddot{x}_n = F(x_{n+1}-x_n)-F(x_n-x_{n-1}) \tag{1}$$

* Corresponding author.

PII: S0022-5096(00)00026-0

Fig. 1. A mass-spring chain.

where $n=0,\pm1,\pm2,\ldots$, and x_n is the coordinate of the mass number n. The function $F(u)$ characterizes the dependence of the spring force vs. spring elongation. We are interested in the situation when this function is *non-monotone*; namely we consider the following basic model of a spring force

$$f(u)=\begin{cases} ku & \text{if } u<u_c \\ ku-f & \text{if } u>u_c \end{cases} \tag{2}$$

where u_c is some critical elongation. In the range $u<u_c$, as well as in the range $u>u_c$ the force F depends linearly on the elongation u with the same slope k, but at the critical value u_c, the spring force $F(u)$ drops by f units, from the value ku_c to the value ku_c-f (see Fig. 2(a)).

1.2. The phenomenon observed in computer experiments

In computer experiments, we have observed the following waves associated with a phase transition. We have stretched the chain so that the distance between any two adjacent masses is $u_c-\varepsilon$ (ε is a "very small" number), and all masses are at rest; all spring forces have the same value $F(u_c-\varepsilon)$. Because of some "small" fluctuations the elongation of one spring can become greater than u_c, say $u_c+\varepsilon$), and then the masses start moving. Let us outline the numerical results.

In computer experiments, we consider a chain of large number N of masses with initial conditions

$$\begin{aligned} x_n(0) &= \begin{cases} (u_c-\varepsilon)n & \text{if } n\le N/2, \\ (u_c+\varepsilon)+(u_c-\varepsilon)(n-1) & \text{if } n>N/2; \end{cases} \\ \dot{x}_n(0) &= 0 \ (n=1,2,\ldots,N;\ \text{e.g. } \varepsilon=10^{-6}). \end{aligned} \tag{3}$$

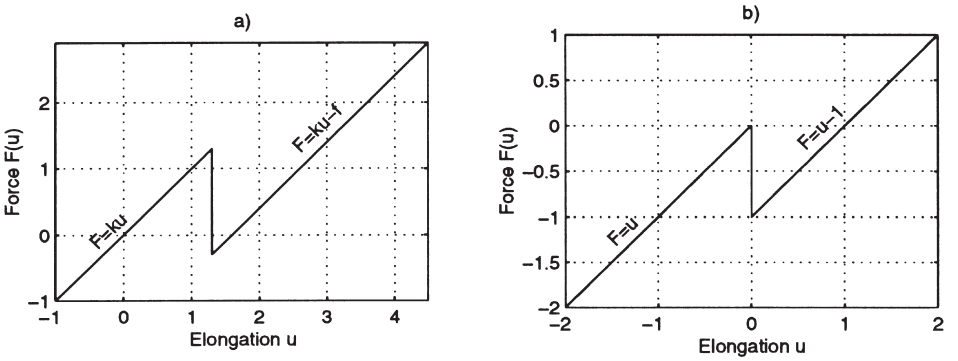

Fig. 2. A model non-monotone constitutive relation (a) characterized by some values of k, u_c and f. (b) normalized to $k=1$, $u_c=0$, and $f=1$.

The result of our computer simulation is shown in Fig. 3. This computation reveals a *phase transition*: the system goes over from one steady state, when the elongation of each spring is constant, to another steady state, when the masses oscillate with some period p. The later phase can be called the *twinkling phase*.

The phase transition propagates symmetrically in opposite directions. This corresponds to the mirror symmetry of the initial conditions Eq. (3).

The phase transition has two fronts. The first one propagates with unit speed (it takes unit time to propagate from one mass to the next). This is the largest speed of propagation of linear waves (see below). Between the first front and the second front, the masses move with "almost" constant speed. After the second front, the masses start to oscillate in a wave motion. Fig. 3 shows several quantitative characteristics of this dynamics. They are as follows.

1. The time period p of the oscillations in the second phase. After the second front the masses start to oscillate in a wave motion with some period p in time.
2. The "swelling" distance α. Before the phase transition the distance between the adjacent masses is (almost) u_c; As a result of the transition the average distance between the adjacent masses becomes equal to $u_c+\alpha$. In other words, as a result of the phase transition, the chain is "swelling" by a distance α, times the number of masses transferred to the twinkling phase.

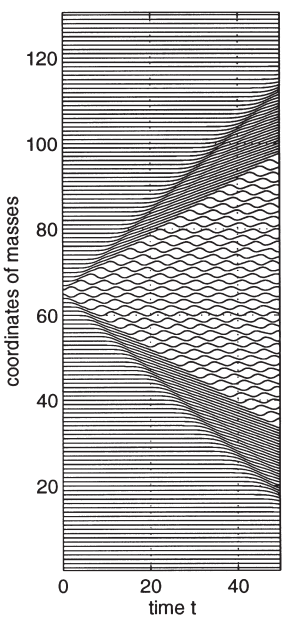

Fig. 3. The result of our computer simulation of the chain with N=130 masses. Initially, the chain is in rest, the distance between any pair of adjacent masses, besides the middle pair, is $u_c-\varepsilon$, and the distance between the two middle masses is $u_c+\varepsilon$ ($\varepsilon=10^{-6}$), so that the chain is "almost" in equilibrium, and its instability "just starts to develop".

3. The speed $1/\tau$ of the second front. After this front the masses start to oscillate. It takes time τ for the second front to propagate from one mass to the next.
4. The speed v in the intermediate regime. Between the first and the second fronts the masses move with a certain "almost" constant speed v.

Our goal is to obtain these characteristics analytically.

1.3. Motivation

This paper continues our previous work (Balk et al., 2000) on the analysis of phase transition in systems with non-convex elastic energy. In numerical experiments, we found quite a regular pattern of phase transition (with two fronts, which propagate with different speeds), and our present goal is to describe this transition.

We note that a similar phenomenon (when a wave of phase transition follows a forerunning sonic or shock wave that has a larger speed) was investigated by Truskinovsky (1997) in a continuous model. Notice that our model describes the oscillations of the twinkling phase, because it possesses internal degrees of freedom (responsible for the oscillations of individual masses).

Another motivation of the work is more general: The Hamiltonian system Eqs. (1) and (2) is interesting from the view point of the general theory of nonlinear waves (see e.g. Whitham, 1993; Infeld and Rowlands, 1990). We have observed a new wave phenomenon (see Fig. 3). Note that the system Eqs. (1) and (2) is *strongly nonlinear*. It does not make sense to consider this system with small force drop f, since it can be always normalized to $f=1$ (see below). An analytical description of this strongly nonlinear system is interesting by itself.

1.4. Normalization

The system Eqs. (1) and (2) can be rescaled to the system, which is characterized by the unit mass $\rho=1$, the unit spring constant $k=1$, zero critical elongation $u_c=0$, and the unit force drop $f=1$. In order to see this, first of all, let us note that the dependence $F(u)$ can be shifted by an arbitrary vector (a,b) in the plane (u,F). Indeed, if we make the following change of variables

$$x_n=\tilde{x}_n+na \ (n=0,\pm1,\pm2,\ldots),$$

then Eq. (1) can be written in the same form, but with a different force

$$\tilde{F}(u)=F(u-a)+b.$$

Therefore, we can shift the dependence $F(u)$ so that the discontinuity occurs at $u_c=0$ and $F(0-)=0$.

Further, we can choose the units of mass so that $\rho=1$, the units of time so that $k/\rho=1$, and the units of length so that $\frac{1}{k}[F(0-)-F(0+)]=1$ (see Fig. 2(b)). Thus we can re-write our system in the form

$$\ddot{x}_n = F(x_{n+1} - x_n) - F(x_n - x_{n-1}) \text{ where } F(u) = u - \Theta(u), \tag{4}$$

where Θ is the Heaviside function.

2. Nonlinear waves

2.1. The formulation

As a first step in the investigation of the system Eq. (4), we find nonlinear waves that can propagate in this system. It is a strongly nonlinear system, and perturbation techniques utilized for finding waves in weakly nonlinear media do not work here.

A somewhat similar system was considered by Slepyan and Troyankina (1984). They studied a mass-spring chain with partially failing bonds. In their model the adjacent masses are joined by two linear springs, and at a certain critical stress one of the springs is torn. In this situation each bond displays nonlinearity only once. On the contrary, each spring in the model considered in this paper is reversible and switches from one linear regime to another infinitely many times.

We look for the solutions $x_n(t)$ of Eq. (4) that are periodic in time

$$x_n(t+p) = x_n(t), \ (n = 0, \pm 1, \pm 2, \ldots; \ -\infty < t < \infty) \tag{5}$$

and satisfy the following self-similarity relation

$$x_{n+1}(t) = \alpha + x_n(t - \tau), \ (n = 0, \pm 1, \pm 2, \ldots; \ -\infty < t < \infty) \tag{6}$$

where p, α and τ are some a priori unknown constants. It is clear that the choice of parameter τ is not unique: the relation Eq. (6) will be satisfied if we replace τ with $\tau + jp$ where j is an arbitrary integer; so we will assume that $|\tau| \le p/2$. Then $|\tau|$ shows how much time it takes for the wave to propagate from one mass to the next, and sign(τ) shows the direction of the wave propagation; in other words $1/\tau$ is the Lagrangian velocity of the wave.

By virtue of the self-similarity property Eq. (6), the coordinates $x_n(t)$ of all the masses can be expressed through the coordinate of only one mass with $n = 0$:

$$x_n(t) = n\alpha + x_0(t - n\tau), \ n = 0, \pm 1, \pm 2, \ldots, \tag{7}$$

Then Eq. (4) takes the following form

$$\ddot{x}_0(t) = F(\alpha + x_0(t - \tau) - x_0(t)) - F(\alpha + x_0(t) - x_0(t + \tau)). \tag{8}$$

We assume that the origin of the x-axis is chosen so that the average value of x_0 is zero:

$$\int_0^p x_0(t)\, dt = 0. \tag{9}$$

2.2. Classes of regimes

The spring force Eq. (4) is piece-wise linear, and the switching from one linear dependence to the other occurs at the instants when the distance between the adjacent masses passes through the critical value u_c=0. For instance, the switching of linear dependence of the first force in Eq. (7) occurs when the function

$$z(t)=x_1(t)-x_0(t)=\alpha+x_0(t-\tau)-x_0(t) \tag{10}$$

passes through zero. The solutions $x_0(t)$ of Eq. (8) can be portioned into several classes depending on how many times the function Eq. (10) changes its sign during the period p.

2.3. Linear waves

If the function Eq. (10) does not change sign at all (it is either everywhere positive or everywhere negative), then Eq. (8) takes the form

$$\ddot{x}_0(t)=x_0(t+\tau)+x_0(t-\tau)-2x_0(t); \tag{11}$$

the mass-spring system behaves as if it were linear. Eq. (11) has solutions

$$x_0(t)=\alpha+Ae^{i\Omega t}, \tag{12}$$

that describe harmonic oscillations. Here the constant A is an arbitrary complex amplitude, and the frequency $\Omega=\dfrac{2\pi}{p}$ is connected with τ by the dispersion relation

$$-\Omega^2=e^{i\Omega\tau}+e^{-i\Omega\tau}-2,$$

which is equivalent to

$$\Omega=\pm 2\sin\frac{\Omega\tau}{2}. \tag{13}$$

Note that the slowest oscillations, with Ω=0, have the largest propagation speed $1/\tau$=1. For the linear regime to take place, the amplitude A should be sufficiently small, so that the function Eq. (10) indeed does not change its sign, e.g. $|A|<\alpha/2$.

2.4. A nonlinear regime

Now consider the situation when the function Eq. (10) does change its sign. In the twinkling phase (Fig. 3), the function Eq. (10) periodically changes its sign from "−" to "+" and then from "+" to "−" once per period p. In other words, the distance between any two adjacent masses once per period becomes greater than the critical distance u_c=0, and once per period it becomes smaller than u_c. We chose the zero of the time-axis so that

$$z(t)>0 \text{ if } 0<t<q \text{ and } z(t)<0 \text{ if } q<t<p \tag{14}$$

where q is some instant between 0 and p. (see Fig. 4). This means that the distance between mass #0 and mass #1 is greater than u_c during time intervals $(0,q)$, $(\pm p, \pm p+q)$, $(\pm 2p,\pm 2p+q)$,… and smaller than u_c during time intervals (q,p), $(\pm p+q,\pm p+p)$,$(\pm 2p+q,\pm 2p+p)$,…. The parameters p and q (a prior unknown) determine the instants of switching between the linear regimes of the spring force (see Fig. 2). Now Eq. (8) can be written in the form

$$\ddot{x}_0(t)=[\alpha+x_0(t-\tau)-x_0(t)-g(t)]-[\alpha+x_0(t)-x_0(t+\tau)-g(t+\tau)]$$

where

$$g(t)=\sum_{j=-\infty}^{\infty}[\Theta(t-jp)-\Theta(t-jp-q)]. \tag{15}$$

The consideration of periodic waves enables us to reduce the nonlinear Eq. (8) to a linear equation

$$\ddot{x}_0(t)=x_0(t+\tau)+x_0(t-\tau)-2x_0(t)+g(t+\tau)-g(t) \tag{16}$$

with external forcing $g(t+\tau)-g(t)$. This equation contains two unknown parameters p and q. We will find solutions of this linear equation that depend on undetermined parameters τ, p, q. Then we will require that the function Eq. (10) satisfies the condition Eq. (14), so that the solution is self-consistent: the switching between the linear branches of the spring force occurs at the "right" instants, i.e. at t=0,q; $\pm p$, $\pm p+q$; $\pm 2p$, $\pm 2p+q$; and so on periodically with period p. This will give us a nonlinear algebraic equation for the four parameters τ,p, q, and α.

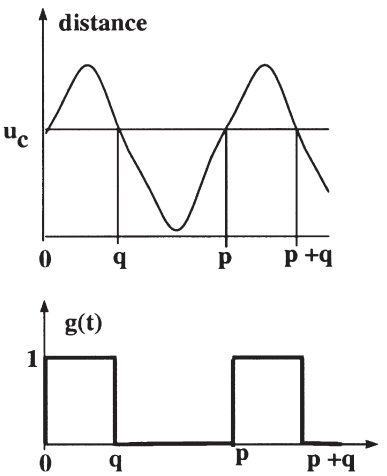

Fig. 4. Switching instances.

2.5. Remark

We wish to emphasize that we are able to reduce the strongly non-linear Eq. (8) to the linear Eq. (16) because we have chosen the dependence $F(u)$ consisting of two linear parts with THE SAME slope (see Fig. 2). Then the nonlinearity is reduced to turning on constant external force at certain instants. If the motion is periodic (and the switching on and off occurs once per period), then the instants of switching (and therefore the external force) are completely characterized by two numbers p and q (see Eq. (15)). In this situation the nonlinear difference–differential Eq. (8) is reduced to the linear difference–differential Eq. (16) and a system of four nonlinear algebraic equations for the parameters τ,p,q, and α.

2.6. The solution of Eq. (16)

We solve the linear difference–differential Eq. (16) by means of Fourier transform similarly to Slepyan and Troyankina (1984). The Fourier series expansion

$$x_o(t)=\sum_{k=-\infty}^{+\infty} X_k e^{ikvt},\ v=2\pi/p, \tag{17}$$

reduces the Eq. (16) to the form

$$(-k^2v^2-e^{ikv\tau}-e^{-ikv\tau}+2)X_k=(e^{ikv\tau}-1)G_k \tag{18}$$

where G_k, is the Fourier coefficient of the function $g(t)$, see Eq. (15):

$$G_k=\frac{1}{p}\int_0^p g(t)e^{-ikvt}\,dt=\frac{1}{2\pi ik}(1-e^{-ikvq}).$$

Hence

$$X_k=\frac{1-e^{-ikvq}}{2\pi ik}\,\frac{e^{ikv\tau}-1}{\left(2\sin\dfrac{kv\tau}{2}\right)^2-(kv)^2},\ v=2\pi/p, \tag{19}$$

($k=\pm1,\pm2,\ldots$; $X_0=0$ according to Eq. (9)) and the solution $x_0(t)$ is given by Eq. (17).

2.7. The nonlinear algebraic equation for the four parameters τ,p,q, and α

We need to ensure that the solution Eqs. (17)–(19) is consistent with the condition Eq. (14), i.e. the function Eq. (10) indeed vanishes at $t=0$ and $t=q$. This means that

$$x_0(t)-x_0(t-\tau)=\sum_{k=-\infty}^{+\infty} X_k(1-e^{-ikv\tau})e^{ikvt} \tag{20}$$

equals α when $t=0$ and $t=q$. Using the solution Eq. (19), we find that condition Eq. (20) gives

$$\text{at } t=0\text{: } \sum_{k=-\infty}^{+\infty} \frac{\sin^2\frac{k\nu\tau}{2}}{\left(\frac{k\nu}{2}\right)^2-\left(\sin\frac{k\nu\tau}{2}\right)^2}\,\frac{1-e^{-ik\nu q}}{2\pi ik}=\alpha$$

$$\text{at } t=q\text{: } \sum_{k=-\infty}^{+\infty} \frac{\sin^2\frac{k\nu\tau}{2}}{\left(\frac{k\nu}{2}\right)^2-\left(\sin\frac{k\nu\tau}{2}\right)^2}\,\frac{e^{ik\nu q}-1}{2\pi ik}=\alpha$$

(in these sums $k\neq 0$).

The sum of these equations gives us the expression for α in terms of the parameters τ,p,q:

$$\alpha=\sum_{k=1}^{\infty} \frac{\sin^2\frac{k\nu\tau}{2}}{\left(\frac{k\nu}{2}\right)^2-\left(\sin\frac{k\nu\tau}{2}\right)^2}\,\frac{\sin k\nu q}{\pi k} \quad (\nu=2\pi/p), \tag{21}$$

while the difference of these equations is satisfied identically (since the resulting summand is odd with respect to the index k).

Thus we have found a three-parameter family[1] of nonlinear waves: Given τ,p,q, we can find α by Eq. (21) and the corresponding nonlinear wave — by formulas Eqs. (17) and (19). Note that in the linear regime we also have three-parameter family of waves, but in this case τ and p are connected by the dispersion relation Eq. (13), and the independent parameters are p,A,α.

It is instructive to compare the waves of described here with water waves, which are characterized by the wave length λ and wave amplitude A (see e.g. Whitham, 1993). The time period p is similar to the wave length λ. The parameter q plays the part of the wave amplitude (it characterizes the nonlinearity). In the present model we have additionally the third parameter α (the average distance between masses), which has no analog for water waves. This parameter arises because we can pre-stretch the chain (before exciting the oscillations). We call the relation Eq. (21) the *nonlinear dispersion relation* for the nonlinear waves in our model.

3. Transition from the stationary phase to the twinkling phase

The wave motion in our computer experiment appears to be a nonlinear wave defined by the formulas Eqs. (7, 17, 19) and (21). However, we have a three-parameter family of nonlinear waves, while our computer experiment is well reproduced

[1] The phase of the wave is the fourth parameter (related to the choice of an initial instant t_0) that we do not count.

and always leads to a *unique* nonlinear wave of the twinkling phase. It remains to be determined which wave from this family describes the wave motion in the computer experiment.

In this section we will show that the values of the parameters p,q,τ are uniquely determined by the condition that the corresponding nonlinear wave is caused by the phase transition. In other words, we describe the entire transition pattern, shown in Fig. 3; the parameters p,q,τ are uniquely determined from the condition that the twinkling phase can be matched with the stationary phase. This assumption corresponds to the wave motion in the twinkling phase and is in agreement with the "experimental" results, Fig. 3.

3.1. Reduction to the linear difference–differential equation with undetermined parameters

The Eq. (4) of the mass spring chain can be written in the form

$$\ddot{x}_n=(x_{n+1}-x_n-g_n)-(x_n-x_{n-1}-g_{n-1}) \tag{22}$$

where

$$g_n=\Theta(x_{n+1}-x_n)\ (n=0,\pm1,\pm2,\ldots). \tag{23}$$

In accordance with our computer experiment, we consider zero initial conditions:

$$x_n(0)=\dot{x}_n(0)=0,\ n=0,\pm1,\pm2,\ldots$$

and assume that the phase transition propagates symmetrically so that

$$x_{1-n}=x_n\Rightarrow g_{-n}=g_n. \tag{24}$$

Let us choose the zero of the time-axis t so that the quantity $x_2(t)-x_1(t)$ is less than zero when $t<\tau$, and it becomes positive for the first time when $t=\tau+$. Fig. 3 suggests that behind the second front the masses move periodically with some period p

$$x_n(t+p)=x_n(t)\ \text{ for }\ t>\tau n \tag{25}$$

in a wave motion with some wave speed $1/\tau$

$$x_{n+1}(t)=\alpha+x_n(t-\tau)\ \text{ for }\ t<\tau n \tag{26}$$

($n=1,2,\ldots$). In the previous consideration of nonlinear waves (Section 2) we required that these relations hold for all $t\in(-\infty,\infty)$. This time we take into account the instant of excitation of the wave and consider the Eqs. (25) and (26) only for $t>\tau n$.

The difference $x_2(t)-x_1(t)$ remains negative up to the instant $t=\tau$; then it becomes positive and stays positive for some time $q(0<q<p)$, i.e. during time interval $(\tau,\tau+q)$; then, at instant $\tau+q$ it becomes negative again and stays negative during time interval $(\tau+q,\ \tau+p)$. After that it repeats periodically with period p. By virtue of the self-similarity condition Eq. (26) we have that

$$x_{n+1}(t)-x_n(t)\begin{cases}<0 \ \text{ if } \ t<\tau|n|,\\ >0 \ \text{ if } \ \tau|n|+pj<t<\tau|n|+pj+q,\\ <0 \ \text{ if } \ \tau|n|+pj+q<t<\tau|n|+p(j+1)\end{cases} \tag{27}$$

(n=1,2,3,…; j=0,1,2,…). This implies that we know the form of the functions $g_n(t)$ (see Eq. (23)) up to three undetermined parameters p,q,τ:

$$g_n(t)=\sum_{j=0}^{\infty}[\Theta(t-n\tau-jp)-\Theta(t-n\tau-jp-q)]. \tag{28}$$

This expression is valid for positive integers (n=1,2,3,…). By virtue of the symmetry Eq. (24), we have a similar expression for $g_n(t)$ with negative n (n=−1, −2, −3,…).

The case n=0 is special since 0th and 1st masses move symmetrically; the sign of $x_1(t)-x_0(t)$ is described by two additional parameters τ_0 and q_0:

$$x_1(t)-x_0(t)\begin{cases}<0 \ \text{ if } \ t<\tau_0,\\ >0 \ \text{ if } \ \tau_0+pj<t<\tau_0+pj+q_0,\\ <0 \ \text{ if } \ \tau_0+pj+q_0<t<\tau_0+p(j+1),\end{cases} \tag{29}$$

and therefore

$$g_0(t)=\sum_{j=0}^{\infty}[\Theta(t-\tau_0-jp)-\Theta(t-\tau_0-jp-q_0)]. \tag{30}$$

3.2. Remark

A close look at Fig. 2 reveals that the wave motion is approximate: $x_{n+1}(t)$ does not exactly equal $\alpha+x_n(t-\tau)$ for n=1,2,…. The relation Eq. (26) holds only when $n\to\infty$. Therefore, we should have introduced different τ_n and q_n for all n=0,1,2,… (not only the case n=0 is special). Moreover, we will see that the periodicity Eq. (25) is also approximate and seems to hold when $t\to\infty$. However, the numerical experiment shows that the accuracy of the above anzatz Eqs. (25) and (26) is "good", and we assume it.

Similarly to the case of nonlinear waves considered in the previous section, we reduce the nonlinear system Eq. (22) to a linear form

$$\ddot{x}_n=x_{n+1}+x_{n-1}-2x_n+g_{n-1}(t)-g_n(t) \tag{31}$$

with the forcing depending on undetermined parameters. This time we need five parameters τ,p,q,τ_0,q_0 instead of three parameters τ,p,q utilized in the case of nonlinear waves, extended from $x=-\infty$ to $x=+\infty$ (see Section 2).

First, we find the solution of the linear system Eq. (31) in terms of the parameters τ,p,q,τ_0,q_0. Then we require that the conditions Eqs. (27) and (29) are satisfied, so that the solution is self-consistent. To do this, we have the five undetermined parameters. However (unlike to the case of nonlinear waves, extended from $x=-\infty$ to $x=+\infty$), it turns out to be impossible to choose the values of the parameters to satisfy all these conditions exactly (because the assumptions of periodicity and wave motion are approximate, see the last remark). Instead, we satisfy these conditions approximately. In this way we obtain a model Eq. (31) that captures the essential features of the phase transition dynamics and agrees with the numerics. This model leads to a unique choice of the values of parameters τ,p,q,τ_0,q_0, and therefore to a unique nonlinear wave of the twinkling phase. The model represents an anzatz, not an approximation based on a small parameter. In this respect our model is similar to a variational approach, when a suboptimal solution is used instead of a "true" minimizer. The comparison with the computer experiment justifies the model.

3.3. Solution of Eq. (31)

To solve the linear Eq. (31), we use the Laplace transform with respect to the time t and the Fourier transform, or z-transform, with respect to the index n.

The Laplace transform

$$X_n(s)=\int_0^\infty x_n(t)e^{-st}\,dt,\ G_n(s)=\int_0^\infty g_n(t)e^{-st}\,dt$$

leads to the equation

$$s^2X_n=X_{n+1}+X_{n-1}-2X_n+G_{n-1}(s)-G_n(s)\ \ (n=0,\pm1,\pm2,\ldots) \tag{32}$$

where

$$G_n(s)=\frac{1-e^{-qs}}{s(1-e^{-ps})}e^{-\tau ns},\ G_{-n}(s)=G_n(s)\ \ (n=1,2,3,\ldots)$$

and

$$G_0(s)=\frac{1-e^{-q_0s}}{s(1-e^{-ps})}e^{-\tau_0 s}$$

The Fourier transform with respect to the index n (z-transform)

$$X(\phi,s)=\sum_{n=-\infty}^{+\infty}X_n(s)e^{in\phi},\ G(\phi,s)=\sum_{n=-\infty}^{+\infty}G_n(s)e^{in\phi}$$

reduces the Eq. (32) to the form

$$(s^2-e^{-i\phi}-e^{i\phi}+2)X(\phi,s)=(e^{i\phi}-1)G(\phi,s) \tag{33}$$

where

$$G(\phi,s)=\frac{1}{s(1-e^{-ps})}\times\left\{(1-e^{-qs})\left[\frac{e^{-\tau s+i\phi}}{1-e^{-\tau s+i\phi}}+\frac{e^{-\tau s-i\phi}}{1-e^{-\tau s-i\phi}}\right]+(1-e^{-q_0 s})e^{-\tau_0 s}\right\} \tag{34}$$

To complete the solution we need to apply the inverse integral transforms.

3.4. Inverse z-transform

From Eqs. (33) and (34) we find $X(\phi,s)$ and then find $X_n(s)$ performing the inverse Fourier transform. Let us consider $n\geq 1$ (the masses with $n\leq 0$ move symmetrically, see Eq. (24)) and make the substitution $z=e^{-i\phi}$; then

$$X_n(s)=\frac{-1}{s(1-e^{-ps})}\times\frac{1}{2\pi i}\oint\left\{(1-e^{-qs})\left[\frac{1}{z-e^{-\tau s}}+\frac{z}{1-ze^{-\tau s}}\right]+(1-e^{-q_0 s})e^{-\tau_0 s}\right\}\frac{(z-1)z^{n-1}\,dz}{z^2-(s^2+2)+1} \tag{35}$$

where the integration is carried out along the unit circle clockwise. In order to calculate this integral, we find the singularities of the integrand.

The quadratic equation

$$z^2-(s^2+2)z+1=0 \tag{36}$$

has two roots whose product is one. This equation has a root with absolute value one only when $\Re(s)=0$ and $-2<\Im(s)<2$. Let $\zeta(s)$ denote the root of Eq. (36) whose absolute value is less than one when $\Re(s)>0$:

$$\zeta(s)=\frac{s^2+2-s\sqrt{s^2+4}}{2} \tag{37}$$

(here we consider the principal value of the square root, with argument between $-\pi/2$ and $\pi/2$); $1/\zeta(s)$ is the other root, whose absolute value is greater than one when s is in the right half-plane. Thus, when $\Re(s)>0$, the integrand in Eq. (35) has two poles inside the unit circle: $z=\zeta(s)$ and $z=e^{-\tau s}$, and we find

$$X_n(s)=\frac{1-e^{-qs}}{s(1-e^{-ps})}\frac{\zeta(s)}{[\zeta(s)-e^{-\tau s}][\zeta(s)-e^{\tau s}]}\left\{(e^{\tau s}-1)e^{-n\tau s}+\frac{2e^{-\tau s}-\zeta(s)-1/\zeta(s)}{\zeta(s)+1}[\zeta(s)]^n\right\}+\frac{1-e^{-q_0 s}}{s(1-e^{-ps})}e^{-\tau_0 s}\frac{[\zeta(s)]^n}{\zeta(s)+1} \tag{38}$$

($n=1,2,\ldots$). These functions are analytic in the right half-plane $\Re(s)>0$. Indeed, when

$\Re(s)>0$, we have $|\zeta(s)|<1, |e^{\tau s}|>1$, so that the denominator in Eq. (38) vanishes only when $\zeta(s)=e^{-\tau s}$, but then the expression in parentheses also vanishes. This analyticity implies that $x_n(t)=0$ when $t<0$ ($n=0,1,2,\ldots$).

In the right half-plane, $\Re(s)>0$, we have $|\zeta(s)|<1$ and $|e^{-\tau s}|<1$; therefore, $X_n(s)\to 0$ and $x_n(t)\to 0$ when $n\to\infty$. This limiting behavior corresponds to the motion of distant masses that at the instant t are not yet reached even by the first front.

3.5. Remark about analytical continuation

The functions Eq. (38) can be analytically continued to the entire complex plane, besides cuts and poles on the imaginary axis. Indeed, the function $\zeta(s)$ can be analytically continued to the entire complex plane with cuts

$$\{s:\Re(s)=0,\ \Im(s)>2\} \text{ and } \{s:\Re(s)=0,\ \Im(S)<-2\}. \tag{39}$$

Then the functions $X_n(s)$ can be meromorphically continued to the complex plane with cuts Eq. (39). The formula Eq. (37) with principal value of the square root actually gives this analytical continuation.

3.6. The asymptotic periodicity of $x_n(t)$ as $t\to\infty$. The choice of parameter q

The asymptotics of $x_n(t)$ when $t\to\infty$ are determined by the singularities of $X_n(s)$ on the imaginary axis. These are the poles at the points

$$s=i\nu \text{ where } \nu=\frac{2\pi}{p}k \ (k=0,\pm1,\pm2,\ldots), \tag{40}$$

as well as at the points of the imaginary axis where

$$\zeta(s)=e^{\tau s}. \tag{41}$$

The last equation has solutions $s=i\Omega$ where $\Omega=\Omega(\tau)$ is a real non-zero roots of the Eq. (13). Note that at $s=0$ the expression Eq. (38) has a simple pole included in the set Eq. (40). Thus,

$$x_n(t)\sim \sum_{k=-\infty}^{\infty} C_k e^{i\frac{2\pi}{p}kt}+[De^{i\Omega t}+D^*e^{-i\Omega t}] \ (t\to\infty) \tag{42}$$

where C_k, ($k=0,\pm1,\pm2,\ldots$; $C_k=C^*_{-k}$) are the residues corresponding to the poles Eq. (40)), and D, D^* are the residues corresponding to the non-zero solutions $s=\pm i\Omega(\tau)$ of Eq. (13).[2] Besides these poles, the analytic functions Eq. (38) have cuts Eq. (39) on the imaginary axis and "one over square-root singularities" at the points $s=\pm 2i$ (since $\zeta(s)+1$ vanishes at $s=\pm 2$ as $\sqrt{s\mp 2}$). These integrable singularities, as well as the cuts, contribute to the asymptotics of $x_n(t)$ at $t\to\infty$. However, these contributions

[2] We have assumed implicitly that Eq. (13) has exactly one pair of non-zero solutions $\pm\Omega(\tau)$, which is true only for some range of τ. The value of parameter τ in our computer experiment is clearly inside this range.

approach zero as $t\to\infty$. Hence the asymptotics of $x_n(t)$ at $t\to\infty$ are determined only by the poles of $X_n(s)$ on the imaginary axis, and we indeed have Eq. (42). The asymptotic Eq. (42) shows that $x_n(t)$ becomes p-periodic as $t\to\infty$ only if $D=0$.

In turn this is realized if q takes some special value so that the factor $1-e^{-qs}$ in the numerator of Eq. (38) vanishes at all zeros of the factor $[\zeta(s)-e^{\tau s}]$ in the denominator. This condition, which could be called the *pole cancellation condition*, gives a relation between the parameter q and τ:

$$q\Omega(\tau)=2\pi \text{ where } \Omega(\tau) \text{ is the positive solution of the equation (13).} \tag{43}$$

In our computer experiment we find $\tau=2.2\Rightarrow\Omega=1.8$ and $q=3.4$, which are in agreement with Eq. (43).

3.7. The "swelling" distance α

The average value of $x_n(t)$ as $t\to\infty$ is determined by the residue of $X_n(s)$ at $s=0$. Thus

$$x_n(t) \text{ oscillates around } \alpha(n-\frac{1}{2})+\beta \text{ as } t\to\infty. \tag{44}$$

Here

$$\alpha=\frac{q\tau}{p(1+\tau)},\ \beta=\frac{q-q_0}{2p}. \tag{45}$$

According to Eq. (44), the constant α is the average distance between adjacent masses, i.e. α is "the swelling distance". In our computer experiment we find $q=3.4$, $\tau=2.2$, $p=5.3$ and $\alpha=0.44$, which fits the theoretical result Eq. (45).

3.8. Solution near the front of the phase transition

In order to obtain the characteristics of the phase transition (in particular the intermediate velocity v between the first and the second fronts), we go over to the frame of reference moving with the front of the phase transition (the second front). In other words, we describe the system using "local" time $\eta=t-n\tau$ (around the instant when the second front reaches mass number n).

We introduce the function

$$y_n(\eta)=x_n(n\tau+\eta)=\frac{1}{2\pi i}\int_{\sigma-i\infty}^{\sigma+i\infty} X_n(s)e^{(n\tau+\eta)s}\,ds= \\ =\frac{1}{2\pi i}\int_{\sigma-i\infty}^{\sigma+i\infty} Y_n(s)e^{\eta s}\,ds \tag{46}$$

(σ is an arbitrary positive number, and $X_n(s)$ is defined in Eq. (38)). According to Eq. (38) we have

$$Y_n(s)=Y(s)+Z(s)[\zeta(s)e^{\tau s}]^n, \tag{47}$$

where

$$Y(s)=\frac{(1-e^{-qs})(1-e^{\tau s})}{s(1-e^{-ps})(e^{-\tau s}+e^{\tau s}-s^2-2))},\ Z(s)=\frac{1}{s(1-e^{-ps})}\left[\frac{(1-e^{-qs})(s^2+2-2e^{-\tau s})}{e^{-\tau s}+e^{\tau s}-s^2-2}+(1-e^{-q_0 s})e^{-\tau_0 s}\right]\frac{1}{\zeta(s)+1}. \tag{48}$$

Here we have taken into account that $\zeta(s)$ and $1/\zeta(s)$ are the roots of the Eq. (36), so that their sum is s^2+2, and therefore,

$$\frac{\zeta(s)}{[\zeta(s)-e^{-\tau s}][\zeta(s)-e^{\tau s}]}=\frac{1}{e^{-\tau s}+e^{\tau s}-(s^2+2)}.$$

In the new frame the self-similarity property Eq. (26) takes the form

$$y_{n+1}(\eta)=\alpha+y_n(\eta)\ \text{ for }\ \eta>\tau n. \tag{49}$$

3.9. The transformation of the integration contour in the inverse Laplace transform

Our idea now is to transform an integration line in Eq. (46) to some path C on which $|\xi(s)e^{\tau s}|<1$, so that the second term in the right hand side of Eq. (47) goes away as $n\to\infty$. In the vicinity of the imaginary axis, when $s=\sigma+i\omega$ (σ being small), we have

$$|\zeta(s)e^{\tau s}|=\begin{cases}1+\sigma\left(\tau-\dfrac{2}{\sqrt{4-\omega^2}}\right)+O(\sigma^2) & \text{if } |\omega|<2(\sigma\to 0),\\[2ex] \dfrac{\omega^2}{2}-\dfrac{|\omega|}{2}\sqrt{\omega^2-4}+O(\sigma)<1 & \text{if } |\omega|>2(\sigma\to+0).\end{cases}$$

Here in the first asymptotics the parameter σ can approach zero from both sides (positive and negative, while in the second asymptotics σ can approach zero only from the positive side. Thus $|\zeta(s)e^{\tau s}|<1$ on the path C shown in the Fig. 5. This path goes along the imaginary axis from $-i\infty$ to $+i\infty$. Whether the path goes to the left or to the right of the imaginary axis is determined by the constant

$$h=2\sqrt{1-\frac{1}{\tau^2}}. \tag{50}$$

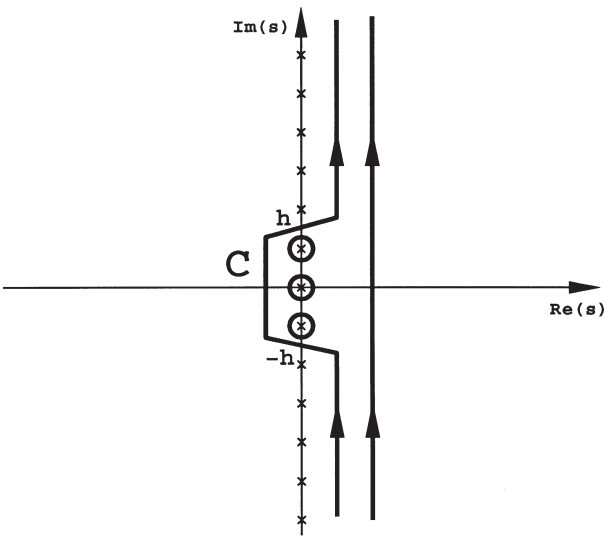

Fig. 5. The line $\Im(s)=\sigma$ of integration in Eq. (46) is transformed to the path C. This path lies near the imaginary axis, in the right half-plane if $|\omega|>h$ and in the left half-plane if $|\omega|<h$. The poles Eq. (40) are denoted by crosses. Three of these poles, $s=0$, $s=iv$, $s=-iv$, lie to the right of C, and the rest lies to the left of C.

If $|\omega|<h$, the path C goes on the left of the axis; if $|\omega|>h$, it goes on the right of the axis. Denoted by crosses in the Fig. 5 are the poles Eq. (40) of the functions $Y_n(s)$ (or $X_n(s)$). According to our computer experiment (Fig. 3), $\tau=2.2\Rightarrow h=1.8$ and $p=5.3\Rightarrow v=2\pi/p=1.2$; therefore three of the poles Eq. (40) lie to the right of the path C, and the rest lies to the left of C. The path of integration in Eq. (46) can be transformed: instead of the straight line from $\sigma-i\infty$ to $\sigma+i\infty(\sigma>0)$ we can integrate over the path C, plus the integrals along the small circles (counterclockwise) around the three poles that lie to the right of C (see Fig. 5); the latter are given by the corresponding residues:

$$y_n(\eta)=\frac{1}{2\pi i}\int_C Y_n(s)e^{s\eta}\,ds+\mathrm{res}_{s=0}[Y_n]+e^{iv\eta}\mathrm{res}_{s=iv}[Y_n]+e^{-iv\eta}\mathrm{res}_{s=-iv}[Y_n]. \tag{51}$$

When $n\to\infty$, the function $Y_n(s)$ on the path C approaches $Y(s)$ and becomes independent of the index n. The second term in Eq. (51) is

$$\mathrm{res}_{s=0}[Y_n(s)]=\alpha(n-\frac{1}{2})+\beta \tag{52}$$

(cf. Eq. (44)).

In order for the self-similarity property Eq. (49) to take place, the last two terms in Eq. (51) should be independent of the index n: It means that the factor $Z(s)$ in Eq. (47) should vanish at $s=\pm iv$:

$$\frac{(1-e^{-iv q})(2-v^2-2e^{-iv\tau})}{e^{-iv\tau}+e^{iv\tau}+v^2-2}=-(1-e^{-iv q_0})e^{-iv\tau_0}. \tag{53}$$

We can satisfy this complex-valued equation by choosing the appropriate values of the two real parameters τ_0 and q_0. Thus, asymptotically as $n\to\infty$ the formula Eq. (51) takes the form

$$y_n(\eta)=\frac{1}{2\pi i}\int_C Y(s)e^{s\eta}\,ds+[\alpha(n-\frac{1}{2})+\beta]+e^{iv\eta}\mathrm{res}_{s=iv}[Y]+e^{-iv\eta}\mathrm{res}_{s=-iv}[Y].$$

Combining together the integral term and the last two residual terms, we rewrite this formula in the form

$$y_n(\eta)=\frac{1}{2\pi i}\int_\Gamma Y(s)e^{s\eta}\,ds+\alpha(n-\frac{1}{2})+\beta \tag{54}$$

where Γ is the path shown in Fig. 6 it goes from $-i\infty$ to $+i\infty$ near the imaginary axis passing all the poles Eq. (40) of the function Eq. (48) on the right, besides one pole at the origin, which is passed on the left. Eq. (54) describes a self-similar behavior of the chain near the front of phase transition, for large n.

3.10. Remark about the self-similar solution near the front of the phase transition

We could look for the solution near the front of the phase transition directly, assuming the self-similarity of this solution:

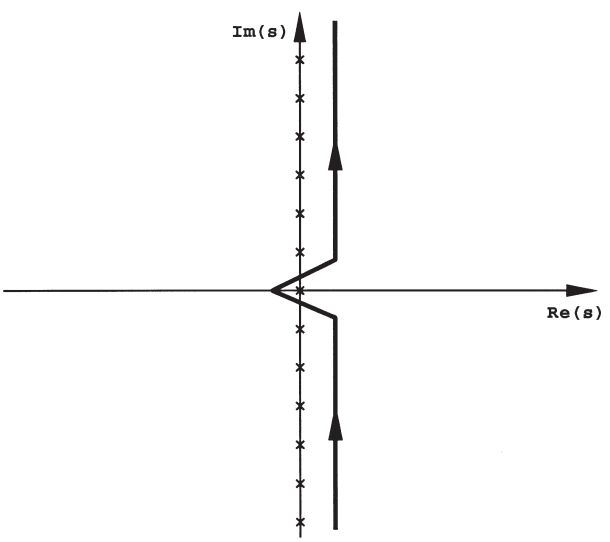

Fig. 6. The path Γ. It lies near the imaginary axis; all the poles Eq. (40) lie to the left of Γ, besides one pole at $s=0$ that lies to the right of Γ.

$$x_n(t)=y(t-n\tau),$$

where τ is an undetermined parameter, and $y(\eta)$ is a p-periodic function. For this function we would derive the following equation

$$\ddot{y}(\eta)=y(\eta+\tau)+y(\eta-\tau)-2y(\eta)+[g(\eta+\tau)-g(\eta)]$$

where

$$g(\eta)=\sum_{j=0}^{\infty}[\Theta(\eta-jp)-\Theta(\eta-jp-q)]$$

(cf. Eqs. (15, 16, 28) and (31)). For the Laplace transform of the function $y(\eta)$ we would find the expression Eq. (48). However, it would be unclear what contour we should take in the inverse Laplace transform. Our approach enabled us to derive the formula Eq. (54) with the integration over contour Γ, shown in Fig. 6). We also showed the necessity of two extra parameters τ_0 and q_0, which describe the dynamics of the middle spring.

3.11. The speed v in the intermediate regime

In order to find the speed v between the first and second fronts (see Fig. 3), we consider the asymptotics of the solution Eq. (54) as $\eta\to-\infty$. It is defined by the pole of $Y(s)$ at $s=0$:

$$Y_s=\frac{1\quad q\tau}{s^2p(\tau^2-1)}[1+s(p+\tau-q)]+O(1)\ \ (s\to 0).$$

Therefore

$$y_n(\eta)\sim v\eta+n\alpha+\gamma \text{ as } \eta\to-\infty$$

where the speed v is

$$v=\frac{q\tau}{p(\tau^2-1)}, \tag{55}$$

$\gamma=v(p+\tau-q)+\beta$ and the constants α and β are defined in Eq. (45). Comparing the expression Eq. (55) for the intermediate speed and the expression Eq. (45) for the "swelling" distance α, we obtain the *kinematic relation*

$$v(\tau-1)=\alpha, \tag{56}$$

which has the following simple kinematic interpretation. It takes unit time for the first front to propagate from mass number n to the mass number $(n+1)$; after this front the masses start moving with the speed v. It takes time $\tau>1$ for the second front to propagate from mass number n to the mass number $(n+1)$; after this front each mass oscillates around a fixed coordinate $n\alpha+\beta$. Thus the mass number $(n+1)$ is moving with the speed v by time $\tau-1$ longer than the mass number n, which is expressed by the relation Eq. (56).

It also follows from the formula Eq. (54) that the masses "almost" do not oscillate between the fronts, which is consistent with Fig. 3. Indeed, the asymptotics $y(\eta)$ as $\eta\to-\infty$ is defined by the singularities of $Y(s)$ that lie on the imaginary axis and are located to the right of the path Γ; there is only one such singularity — $s=0$ (and there are no singularities with non-zero imaginary part, which would lead to oscillations).

3.12. Parameters p and τ. The nonlinear dispersion relation

Up to now we did not fix the values of the two parameters p and τ. We need to choose these values to make our solution self-consistent: We require that the distance between masses number n and number $(n+1)$ vanishes (and switching between linear regimes of the spring force indeed occurs) at the "right" instants. Namely

$$x_{n+1}(t)-x_n(t)=0 \quad \text{when } t=n\tau+pj \quad \text{and} \quad t=n\tau+pj+q \tag{57}$$

($n=1,2,3,\ldots$; $j=0,1,2,\ldots$; cf. Eq. (27)). The Laplace transform $X_n(s)$, given by the formula Eq. (35); is not a meromorphic function, and therefore, the solution $x_n(t)$ cannot be periodic. It is impossible to satisfy Eq. (57) exactly. However, the computer experiment suggests that $x_n(t)$ is periodic with sufficiently high accuracy. We satisfy the condition Eq. (57) approximately, and moreover consider this condition for large n, when we can use the asymptotic formula Eq. (54). Since $y_n(\eta)=x_n(n\tau+\eta)$, we have

$$x_{n+1}(n\tau+\eta)-x_n(n\tau+\eta)=\frac{1}{2\pi i}\int_\Gamma Y(s)(e^{-\tau s}-1)e^{s\eta}\,ds+\alpha.$$

Therefore, the condition Eq. (57) takes the form

$$\frac{1}{2\pi i}\int_\Gamma Y(s)(e^{-\tau s}-1)e^{s\eta}\,ds+\alpha=0 \tag{58}$$

for instants

$$\eta=pj,\ \eta=pj+q \quad (j=0,1,2,\ldots). \tag{59}$$

We satisfy this condition asymptotically for instants Eq. (59) as $j\to\infty$. Asymptotics of $y_n(\eta)$ as $\eta\to+\infty$ are determined by the poles Eq. (40), and we find that as $\eta\to+\infty$, the chain performs the wave motion described by the formulas Eqs. (17) and (19). Hence we arrive at the nonlinear dispersion relation Eq. (21) (see Section 2). Since the parameter α is given now by the formula Eq. (45), the dispersion relation represents an equation connecting the wave period p, the wave speed $1/\tau$, and the parameter q (the latter plays the part of the wave amplitude).

The asymptotic considerations of this section give us three equations for the four parameters p,q,τ, and α. We also need to require that the condition Eq. (57) holds at $t=\tau n$, i.e. the wave of phase transition indeed reaches the mass number n at the instant $t=n\tau$ (see Eq. (27)). This condition is the Eq. (58) with $\eta=0$:

$$\frac{1}{2\pi i}\int_{\Gamma}\frac{(1-e^{-qs})(1-e^{\tau s})(e^{-\tau s}-1)}{(1-e^{-ps})(e^{-\tau s}+e^{\tau s}-s^2-2))}\,ds+\alpha=0. \tag{60}$$

It represents the fourth equation for the four parameters p,q,τ and α.

4. Conclusion

In computer experiments we found a new regular pattern of dynamical phase transition in the mass-spring chain (see Fig. 3). The phase transition has two fronts propagating with different speeds. Due to this transition the mass-spring chain transfers from the stationary state, when all the masses are at rest, to the twinkling state, when the masses perform a wave motion. The pattern is well reproduced and is characterized by several quantitative characteristics, e.g. (1) the time period p of waves, (2) the "swelling" distance α, (3) the speed $1/\tau$ of the second wave front, (4) the intermediate speed v (see the end of Section 1).

In order to approach this strongly nonlinear system analytically, we have found the special form of the force vs. elongation dependence (see Fig. 2); the dependence consists of two linear parts with the *same* slope.

We have found analytically a three-parameter family of exact solutions, which represent the nonlinear waves (extending from $-\infty$ to $+\infty$). The wave motion of the twinkling phase, which we observed in the computer experiment, represents such a nonlinear wave. (One would observe this nonlinear wave if he is in "the middle" of the twinkling phase and knows nothing about the boundaries, as well as about the "pre-history".)

A natural question arises: "What particular wave out of that three-parameter family of nonlinear waves is realized in computer experiment?" In order to answer this question, we have considered the entire transition dynamics. This has lead us to the system of algebraic equations for the parameters p,τ,α and a certain parameter q. The latter is similar to the wave amplitude in the general theory of nonlinear waves; it indicates the instants of switching between the linear parts of the force dependence.

We summarize here the main steps in the derivation of this nonlinear system.

1. We require that the solution that we construct is asymptotically time-periodic as $t\to+\infty$. This is possible only if a certain cancellation of poles of the image Eq. (38) occurs. This requirement (the pole cancellation condition, see Section 3) gives us the Eq. (43), which determines q in terms of parameters τ:

   $$q\Omega(\tau)=2\pi, \tag{61}$$

   where $\Omega(\tau)$ is defined by the linear dispersion relation Eq. (13): $\Omega(\tau)$ is the positive root of the equation

   $$\Omega=2\sin\frac{\Omega\tau}{2}.$$

2. We consider the asymptotics of our solution as $t\to+\infty$ and find "the swelling distance" α in terms of the parameters p,q,τ (Eq. (45)):

$$\alpha=\frac{q\tau}{p(1+\tau)}. \tag{62}$$

3. We consider the solution near the second front, propagating with the speed $1/\tau$. Moreover, we consider the asymptotic regime when $n\to+\infty$ and $t\to+\infty$, but $\eta=t-n\tau$ stays finite. The requirement that our solution asymptotically represents a self-similar wave defines the parameters τ_0 and q_0 (characterizing the dynamics of the "middle" spring, see Eqs. (29) and (53)) and leads to the asymptotic formula Eq. (54):

$$x_n(n\tau+\eta)=\frac{1}{2\pi i}\int_\Gamma Y(s)e^{s\eta}\,ds+\alpha(n-\frac{1}{2})+\beta. \tag{63}$$

Here the function $Y(s)$ is given by Eq. (48):

$$Y(s)=\frac{(1-e^{-qs})(1-e^{\tau s})}{s(1-e^{-ps})(e^{-\tau s}+e^{\tau s}-s^2-2)}, \tag{64}$$

the path Γ is shown in Fig. 6, the "swelling distance" α and the constant β are defined in Eq. (45). The singularities of the function $Y(s)$ on the imaginary axis and the form of the path Γ (see Fig. 6) define the asymptotic behavior of the integral Eq. (63) as $\eta\to\pm\infty$. The behavior at $\eta\to-\infty$ is defined by the only pole to the right of $\Gamma-$ the double pole at $s=0$. We find that when $\eta\to-\infty$, the function Eq. (63) grows linearly with η, and there are no oscillations in the intermediate region, between the fronts. This leads to a simple kinematic expression for the intermediate velocity v

$$v=\frac{\alpha}{\tau-1} \tag{65}$$

(see Eq. (56) and the physical interpretation after that equation).
The simple poles of $Y(s)$, located on the imaginary axis to the left of the path Γ, determine the asymptotic behavior of Eq. (63) at $\eta\to+\infty$: asymptotically solutions $x_n(n\tau+\eta)$ become p-periodic functions and take the form of a nonlinear wave found in Section 2. Thus we have the nonlinear dispersion relation Eq. (21):

$$\alpha=\sum_{k=1}^{\infty}\frac{\sin^2\dfrac{kv\tau}{2}}{\left(\dfrac{kv}{2}\right)^2-\left(\sin\dfrac{kv\tau}{2}\right)^2}\,\frac{\sin kvq}{\pi k}\quad(v=2\pi/p). \tag{66}$$

4. The last equation for the parameters comes from the requirement: $x_{n+1}(n\tau)-x_n(n\tau)=0$. It states that the masses indeed transfer to the twinkling phase when the second front reaches them. Using the asymptotic formula Eq. (63) we arrive at Eq. (60):

$$\frac{1}{2\pi i}\int_{\Gamma}\frac{(1-e^{-qs})(1-e^{\tau s})(e^{-\tau s}-1)}{s(1-e^{-ps})(e^{-\tau s}+e^{\tau s}-s^2-2))}\,ds+\alpha=0. \tag{67}$$

The four Eqs. (61, 62, 66) and (67) define the values of the parameters p,q,τ, and α. Once these parameters are determined, the formulas Eqs. (63) and (64) determine the self-similar wave of phase transition.

4.1. Comparison with numerics

Our analysis is based on the hypothesis that the solution represents wave motion when $t>n$ (i.e. after the front of phase transition has passed the mass). We would like to check this hypothesis not only qualitatively, but also quantitatively. In order to do this, we check that the values of the parameters p,q,τ,α, found in computer simulation, satisfy the four Eqs. (61, 62, 66) and (67). In our computer experiments we found $p=5.3$, $q=3.4$, $\tau=2.2$, $\alpha=0.44$. These values indeed agree (within the measurement accuracy) with the four equations.

4.2. Turbulence

We should note that the regular pattern shown in the Fig. 3 starts to disintegrate after about ten periods of oscillations. If we continue to compute further (beyond the time interval of $t\approx 50$ presented in the Fig. 3), the oscillations become irregular and chaotic. At present we are not sure whether this disintegration is due to the numerics or is inherent to the real nonlinear dynamics. Probably, this disintegration takes place because of the instability of the nonlinear wave (in the oscillating phase). In following papers we intend to describe the developed turbulence of random nonlinear waves in this system.

References

Balk, A.M. Cherkaev, A.V., Slepyan, L.I., 2000. Dynamics of solids with non-monotone stress–strain relations, I. Gibbs principle (in press).

Infeld, E., Rowlands, G., 1990. Nonlinear Waves, Solitons and Chaos. Cambridge University Press.

Slepyan, L.I., Troyankina, L.V., 1984. Fracture wave in a chain structure. Prikl. Mekh. Tekh. Fiz. 6, 128–134.

Truskinovsky, L., 1997. Nucleation and growth in elasticity. In: Duxbury, P., Pence, T. (Eds.), Dynamics of Crystal Surfaces and Interfaces. Plenum Press, New York, pp. 185–197.

Whitham, G.B., 1993. Linear and Nonlinear Waves. Willey Interscience.